Local Motions in a Microphase-Separated Poly(styrene-*b*-methylphenylsiloxane) Diblock Copolymer Melt

S. Vogt, B. Gerharz, and E. W. Fischer

Max-Planck Institut für Polymerforschung, P.O. Box 3148, 6500 Mainz, Germany

G. Fytas*

Foundation for Research and Technology—Hellas, P.O. Box 1527, 71110 Heraklion, Crete, Greece

Received April 22, 1992; Revised Manuscript Received July 7, 1992

ABSTRACT: The segmental dynamics in the microregions of a microphase-segregated poly(styrene-*b*-methylphenylsiloxane) (P(S-*b*-MPS)) with M_n = 59.000 and PS fraction f_{PS} = 0.22 were selectively studied by depolarized light scattering and dielectric spectroscopy over the temperature range −20 to +110 °C. About 50% of the material was found to partition in PS-rich and PMPS-rich environments with orientational dynamics very similar to that of the pure homopolymers. Below the high glass transition temperature, the segmental relaxation within the PS microregion displays a weaker temperature dependence and the relaxation distribution function becomes narrower, as compared to those of PS homopolymer.

Introduction

Diblock copolymer (A–B) melts exhibit several ordered mesophases when the reduced product $\chi(T)N$ between the segment–segment interaction parameter χ and the total degree of polymerization N exceeds a composition (f) dependent value $C(f)$. For example, the mean-field[1] result for symmetric (f = 0.5) A–B is C = 10.5. Microphase segregation (MST) can be achieved by decreasing T, since $\chi \approx 1/T$ or increasing N. Whereas the major part of the published theoretical and experimental work is concerned with the static properties of A–B copolymers,[2] the understanding of their dynamic properties is very limited. In particular, segmental relaxations in disordered A–B melts with different positions in the phase diagram have been very recently considered.[3-5]

Local motions in diblock copolymers are affected by the compositional heterogeneities in the homogeneous melt. Despite the presence of a single glass transition, slow composition fluctuations $\langle\psi^2_q\rangle$ in a microscopic cooperative volume V_c can result in two distinct primary segmental relaxations[6] intermediate between those of the bulk homopolymers. Here ψ_q is the Fourier transform of $\psi(r) = \rho_A(r)/\rho - f$ where $\rho_A(r)$ is the local density of A segments and ρ the overall (A + B) segment density. Surprisingly, athermal (χ = 0) A–B copolymers were also found to exhibit two primary relaxations.[7] The separation of the two processes, as well as the width of the relaxation time distribution, appears to depend on the amplitude $\langle\psi^2_q\rangle$ and the difference in the glass transition temperatures (T_g) of the two blocks. So far, there is no theoretical account for these experimental findings.

Heterogeneous diblock copolymers exhibit two distinct glass transitions very close to the T_g's of the constituent homopolymers.[5] However, the confinement of the subchains in the mesophases is expected to exert profound influence on the characteristics of the segmental relaxations of the subchains as related to the two homopolymers. It has been recently reported[8] that the block overall orientation observed by dielectric spectroscopy (DS) is significantly retarded and broadened as compared to the homopolymer counterpart. In this paper, we employ depolarized Rayleigh scattering (DRS) and DS to investigate, for the first time, local dynamics in the microdomain regions. For this purpose, we have chosen a thoroughly characterized[9] (styrene-*b*-methylphenylsiloxane) (P(S-*b*-MPS)) copolymer with N = 470 and f_{PS} = 0.22. Whereas both PS and PMPS segments possess optical anisotropy ($\langle\gamma^2\rangle_{PS}$ = 38 Å^6 and $\langle\gamma^2\rangle_{PMPS}$ = 28 Å^6) and hence give rise to DRS, the dielectric response of the copolymer originates mainly from PMPS segments.

Experimental Section

Sample. The synthesis and characterization of the P(S-*b*-MPS) sample has been described elsewhere.[9] The total weight-average molecular weight M_n amounts to 5.9 × 10^4 with M_w/M_n = 1.05. Differential scanning calorimetric measurements at a rate 10 K/min clearly show two well-separated glass transitions at +91 and −26 °C with breadth ΔT_g = 50 and 20 K, respectively. The closeness of these values with the T_g's of the bulk PS (T_g = 98 °C, ΔT_g = 18 K) and PMPS (T_g = −28 °C, ΔT_g = 9 K) homopolymers is in accordance with the microdomain structure of the sample. In fact, the MST was determined by dynamic shear mechanical and small-angle X-ray scattering (SAXS) measurements to be 130 °C. The mean-field representation of the correlation peak yields a weak temperature-dependent interaction parameter $\chi = 0.67/T + 0.024$ and radius of gyration R_g = 72 Å. In the strong segregation limit the present sample should form cylindrical microstructures with PS chains in the interior.[2]

Photon Correlation Spectroscopy (PCS). The autocorrelation function $G_{VH}(t)$ of the depolarized light scattering intensity was measured at a scattering angle of 90° using an ALV-5000 full digital correlator over the time range 10^{-6}–10^3 s. The incident laser beam with wavelength λ = 488 nm and single mode intensity 150 m W was polarized perpendicular (V), whereas the polarization of the scattered light was parallel (H) to the scattering plane. The excellent optical quality of the sample—prepared by filtration (0.45-μm millipore filter) directly into the dust-free light scattering cell (o.d.$^1/_2$ in.) at high temperature under pressure—allowed the computation of the desired orientation relaxation function

$$C(t) = [(G_{VH}(t) - 1)/f]^{1/2} \quad (1)$$

under homodyne conditions.[10] The instrumental factor f ($\simeq$0.65) was obtained from the $G_{VV}(q,t)$ of a dilute PS/CCl_4 solution. Dynamic depolarized light scattering within the time window of PCS was displayed by the present sample over the temperature ranges 110–60 °C and −8 to −18 °C.

Dielectric Spectroscopy (DS). The real and imaginary parts of the complex dielectric permitivity ϵ^* were measured from 10^{-1} to 10^6 Hz by using a Solartron-Schlumberger frequency analyzer FRA-1260. The sample was kept between the gold-plated

0024-9297/92/2225-5986$03.00/0

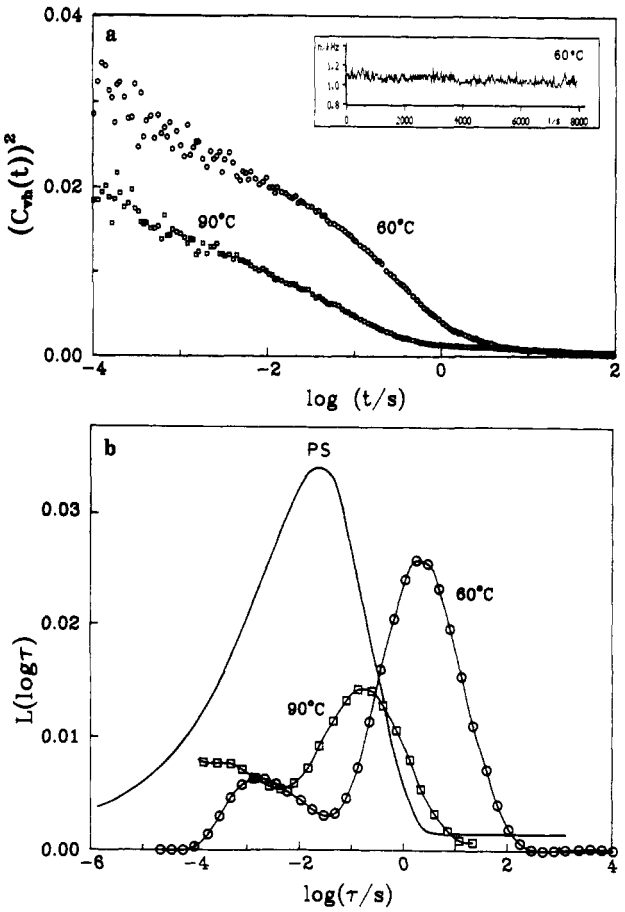

Figure 1. (a) Experimental orientation correlation function $|C(t)|^2$ (eq 1) for the microphase-separated P(S-*b*-MPS) copolymer with $f_{PS} = 0.22$ at two temperatures near the high T_g. The depolarized light scattering intensity profile is given in the inset. (b) Distribution $L(\log \tau)$ of orientation times obtained from the inversion of the time correlation functions of (a). The solid line denotes the $L(\log \tau)$ for the PS homopolymer (arbitrarily shifted on the time axis).

stainless steel electrodes and the temperature varied over the range 0 to −30 °C.

Results

Near the high T_g of the sample, PCS probes the segmental motion of PS under homodyne conditions (eq 1). Figure 1 displays the square of the orientation relaxation function and the corresponding relaxation time distribution function $L(\log \tau)$ at two temperatures. The latter is obtained from the inverse Laplace transform (ILT) of $C(t)$ without an a priori assumption of the form of $L(\log \tau)$ but assuming a superposition of exponentials, in analogy to the treatment of mechanical data.

$$C(t) = \int_{-\infty}^{\infty} L(\ln \tau) e^{-t/\tau} \, d \ln \tau \qquad (2)$$

From the shape of $L(\log \tau)$ it becomes evident that the fit of the common Kohlrausch–Williams–Watts (KWW) decay function $b \exp(-(t/\tau^*)^\beta)$ would display systematic deviations. Here, b is the amplitude, and τ^* and β are the KWW relaxation time and the shape parameter, respectively. In the ILT representation, $b = \int_{-\infty}^{\infty} L(\ln \tau) \, d \ln \tau$. The amplitude b is the fraction of the depolarized light scattering intensity $\langle I_{VH} \rangle$ with correlation times longer than about 10^{-6} s. If the relaxation functions $C(t)$ of Figure 1a originate only from PS segmental orientation, b is estimated to be $\langle \gamma^2 \rangle_{PS} f_{PS} / \sum \langle \gamma^2 \rangle_i f_i \simeq 0.3$ with i = PS or PMPS assuming negligible collective anisotropic scattering. The short time intercept ($b \simeq 0.15$ at 60 °C) of the

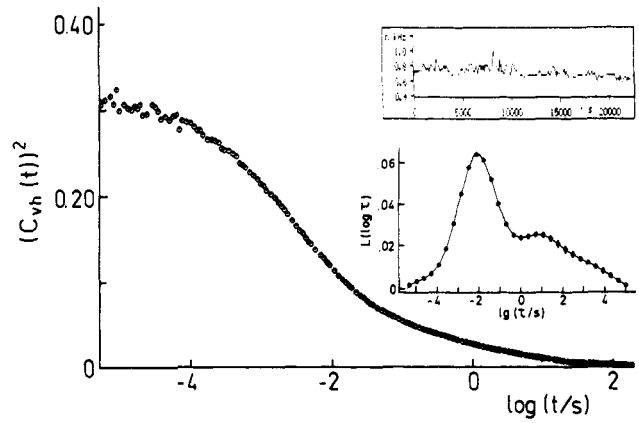

Figure 2. Experimental $|C(t)|^2$ (eq 1) for P(S-*b*-MPS) at −12 °C near the low T_g. The corresponding $L(\log \tau)$ and the intensity profile are given as insets.

$C(t)$ in Figure 1 is even lower for the present sample rich in the PMPS component. That the latter is predominantly responsible for the faster fluctuating fraction of $\langle I_{VH} \rangle$ is mainly evident from the measured orientation function $C(t)$ at much lower T near the second T_g of the sample.

Figure 2 shows the experimental function $C(t)$ at −12 °C along with the corresponding $L(\log \tau)$ (inset). In contrast to Figure 1, $C(t)$ at low T is characterized by a plateau of short times with $b \simeq 0.6$ and a long time tail leading to the second slow peak of $L(\log \tau)$ in Figure 2. Like the main peak of $L(\log \tau)$ in Figure 1, the fast process reflects a moderate distribution of relaxation times; homogeneous block copolymers display extremely broad $L(\log \tau)$.[5-7] In the ILT analysis of $C(t)$ we assumed homodyne conditions and an ergodic medium. While this appears to be the case at high T, the presence of frozen-in orientation fluctuations for PS near the low T_g would in principle act as a local oscillator with intensity I_c. At low T the total intensity $\langle I_{VH} \rangle = I_c + \langle I_F \rangle$ where $\langle I_F \rangle$ denotes the contribution of the fluctuating ($\tau > 10^{-6}$ s) component due to the PMPS segmental orientation dynamics. For this heterodyne case, the desired normalized $C^*(t) = \langle E^*_F(0) E_F(t) \rangle / \langle I_F \rangle$, with E_F being the electric field of depolarized scattered light, enters the expression[11]

$$(G_{VH}(t) - 1)/f = \alpha^2 |C^*(t)|^2 + 2\alpha(1-\alpha) C^*(t) \qquad (3)$$

which should be in contrast to the homodyne equation (eq 1). The measured $(G_{VH}(t) - 1)/f$ has an amplitude $\sigma^2 = \alpha(2-\alpha)$ where $\alpha = \langle I_F \rangle / \langle I_{VH} \rangle$. Since $\alpha < 1$, the amplitude of the correlation function under heterodyne conditions is reduced ($\sigma < 1$).

To proceed with the PCS data reduction near the lower T_g of PMPS in terms of eq 3, we consider first the dielectric loss $\epsilon''(\omega)$ response because it selectively arises from the PMPS subchain and the analysis involves less assumptions. The upper part of Figure 3 depicts the dispersion of $\epsilon''(\omega)$ for the copolymer and the PMPS homopolymer under the same conditions. Both samples clearly display single segmental relaxation peaks with similar widths but show significantly different amplitudes and peak positions. The dielectric strength $\Delta\epsilon$ obtained from the fit of a single Havriliak–Negami (HN)[12]

$$\epsilon^* - \epsilon_\infty = \Delta\epsilon / [1 + (i\omega\tau)^\alpha]^\gamma \qquad (4)$$

plus a conductivity term to the experimental data is lower than expected for weight fraction $w_{PMPS} = 0.79$; the experimental $\Delta\epsilon = 0.16$ should be compared with $\Delta\epsilon(\text{bulk}) \cdot w_{PMPS} = 0.27$. In eq 4, ϵ_∞ is the high-frequency limiting ϵ' and α and γ are parameters ($0 \le \alpha, \gamma \le 1$) describing,

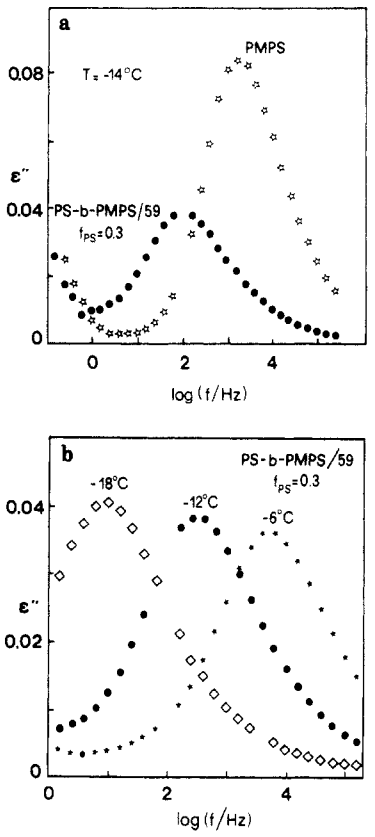

Figure 3. (a) Dielectric loss $\epsilon''(\omega)$ for P(S-*b*-MPS) and the PMPS homopolymer at −14 °C. (b) $\epsilon''(\omega)$ for P(S-*b*-MPS) at different T near the low T_g.

respectively, the symmetric and asymmetric broadening of the distribution. Over the T range 240–340 K, the $\epsilon''(\omega)$ spectra exhibit a single structure as shown also in Figure 3b. This finding suggests the presence of one mobile (10^{-1} s < τ < 10^{-5} s) fraction of PMPS with $f^*_{PMPS} = \Delta\epsilon/\Delta\epsilon$(PMPS) ≃ 0.47 while the slow dynamics of the still missing fraction (~0.32) is not accessible under the present experimental conditions. Of course, this proposition holds for single particle orientation as mentioned for PS previously.

In contrast to the DS data, the $C(t)$ in Figure 2 indicate the presence of two relaxation processes. The fast relaxation time can be compared with the dielectric time; under homodyne conditions (eq 1), the former is by an order of magnitude slower. It also appears (Figure 3b) that the slow process is dielectrically inactive, and hence it cannot be assigned to slow PMPS dynamics at the interface. Instead, the assumption of aggregates or frozen-in orientation fluctuations in the PS microphase could explain the presence of the slow process in the PCS experiment. In this context we should mention that the form of eq 3 cannot create the experimental shape, i.e., a double peak in $L(\log \tau)$, but it does affect the value of the relaxation time. The contribution of two processes, however, would render a fit of eq 3 ambiguous.

For bulk PMPS, DS and PCS experiments analyzed in a consistent way yield the same relaxation parameters.[5] On this premise, we have estimated $\sigma = \langle\gamma^2\rangle_{PMPS} f^*_{PMPS} / \sum\langle\gamma^2\rangle_i f_i = 0.43$. The denominator is the same as before since the total $\langle I_{VH}\rangle$ intensity is more or less constant over the examined T range. This value of σ is about 30% higher than the experimental value (σ = 0.3). The latter is obtained from the plateau of $C(t)$ (Figure 2a) at short times and after subtraction of the slow mode contribution. This reduction in the amplitude σ can be rationalized in terms of eq 3 if $\alpha \simeq 0.5$ and hence $I_c/\langle I_{VH}\rangle \simeq 0.5$ where I_c is the "static" contribution of slow PMPS and PS segmental fluctuations. The profile of I_{VH} (Figure 2) indeed shows such ultraslow fluctuations ($\tau \simeq 2$ h). The fraction $I_c/\langle I_{VH}\rangle$ is roughly the sum of the slow contributions $I_{PS}/\langle I_{VH}\rangle = 0.3$ and $I_{PMPS}/\langle I_{VH}\rangle = 0.25$. Under these conditions simulated functions (eq 3) show that the value of the relaxation time is very close to that obtained in the pure heterodyne limit (only the linear term). The relaxation parameters of the heterogeneous copolymer from DS and PCS experiments are given in Table I.

Discussion

The combination of the two complementary techniques allows the selective study of the segmental dynamics of PS and PMPS in the weakly segregated diblock P(S-*b*-MPS). The preceding analysis led to the characteristic relaxation parameters subject to certain assumptions as stated above. The reduced amplitudes of the two segmental relaxations, the T dependence of the relaxation time, and the corresponding distribution function of the less mobile block (PS) originate probably from the copolymer microstructure. We discuss next these new results in the two microregions.

1. **High T_g Microphase.** PCS above 60 °C measures segmental orientation in the PS-rich environment. This assignment is based on the closeness between the values of the orientation time in the copolymer and bulk PS homopolymer, as shown in Figure 4. Furthermore, neglecting domain versus molecular anisotropic scattering in the weakly segregated sample, the low amplitude of $C(t)$ in Figure 1 corroborates the notion that a fraction of PS segments in the PS microregion undergo slow orientation, being only slightly faster than pure PS. The composition $\Phi_{PS/PS}$ within this region can be estimated from the temperatures at which segmental motion assumes the same relaxation rate or from the T_g's of the pure homopolymers.[9] Both quantities yield $\Phi_{PS/PS} = 0.93$ and $\Phi_{PS/PMPS} = 0.05$ for the PS composition within the PMPS microregion. We should mention that these fractions are referred to the cooperative volume[13] V_c usually invoked for the primary glass process.

Table I
Segmental Relaxation Parameters in P(S-*b*-MPS) Heterogeneous Copolymer

PCS				DS				
T (°C)	β_{KWW}[a]	τ (s)	τ_{max} (s)	T (°C)	α	γ	τ_{HN} (s)	β_{KWW}
110	0.20	9×10^{-3}	2×10^{-3}					
100	0.32	4.9×10^{-2}	7.1×10^{-2}					
90	0.45	1.1×10^{-1}	1.4×10^{-1}					
70	0.56	7.2×10^{-1}	7.9×10^{-1}					
60	0.63	1.6	2.2					
−9	0.40	2×10^{-4}	2.7×10^{-4}	−9	0.6	0.81	9.3×10^{-5}	0.47
−12	0.50	1.9×10^{-3}	2.6×10^{-3}	−12	0.65	0.69	8.5×10^{-4}	0.46
−17	0.47	1.1×10^{-1}	2×10^{-1}	−17	0.69	0.61	9.5×10^{-3}	

[a] β = 0.35 for bulk PS, and β = 0.44 for bulk PMPS.

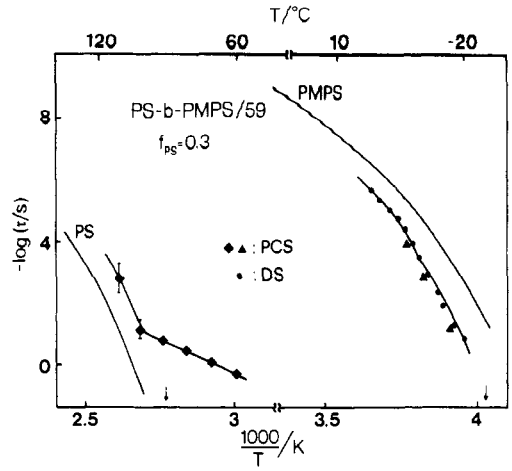

Figure 4. Two different time scales for segmental orientation in PS (◆) rich and PMPS (●,▲) rich microregions of the P(S-*b*-MPS) copolymer over a broad T range. The relaxation times from PCS (●,▲) and DS (●) were obtained from the maximum in $L(\log \tau)$ and HN fits (eq 4) of $\epsilon''(\omega)$, respectively. Solid lines are for the segmental motion in pure homopolymers, and the arrows denote the two T_g's.

The amplitude $b = 0.15$ associated with the relaxation process within the PS microregion is about half of the expected value on the basis of the overall f_{PS}. To rationalize this result, we have estimated the amount of the interfacial material as $2\delta x/L$. Taking the interface width $\delta x \approx 2/q^*$ and the microdomain period $L = 2\pi/q^*$ where $q^* \approx 2/R_g$, the fraction of the material partitioned into the interface is about 60%.[14] Considering the uncertainties in both quantities, the observed agreement is reasonable. The lack of a short time plateau in $C(t)$ of Figure 1 as compared to Figure 2 indicates the presence of faster orientation dynamics due to the PMPS microregion and the interfacial material. Alternatively, the local dynamics of $C(t)$ in Figure 1 originate from virtually pure PS microenvironments ($\sim V_c$); in these subvolumes the participation of PS is about 50%. This picture is also in accord with a stretched copolymer chain consisting of two subchains that are more densely packed than Gaussian coils.[15,16]

Figure 4 displays the T dependence of τ_s obtained from the slow peak of $L(\log \tau)$ in Figure 1. As anticipated from the preceding discussion, τ_s appears to exhibit a similar T dependence with that in bulk PS. In this T region, there exist only two experimental points because of the broad distribution functions involved and the short time edge of PCS. An interesting feature is the appearance of a kink near the high T_g of the sample. Similar T dependence has, for the first time, been observed in a disordered poly(styrene-*b*-isoprene) copolymer melt.[6] Below the high T_g, the increase of τ_s with decreasing T occurs with a significantly lower rate. We attribute this finding to the freezing of free volume V_f in the PS microphase. Furthermore, the experimental observation of this kink in the copolymer but not in the PS homopolymer implies a higher V_f value in the former due to some phase mixing. An alternative explanation based on crystallization, induced by a stretched chain configuration though low (~10% near MST), is probably ruled out on the grounds of X-ray scattering and I_{VH} data.

The width of the segmental distribution function expressed either in terms of β_{KWW} (Table I) or $L(\log \tau)$ (Figure 1) was found to vary with T in contrast to the PS homopolymer melt; for the latter $\beta_{KWW} = 0.35$ over the range T_g to $T_g + 30$ K. Moreover, this variation of the width with T is different above and below the high T_g. Above T_g, we can only qualitatively state that β_{KWW} is somewhat lower than that in bulk PS. In view of previous experience in disordered block copolymer melts[6] we should anticipate rather extensive broadening of the distribution function. Slow composition fluctuations in the microregions can broaden the spectrum of relaxation times. What appears unexpected is the narrowing of the distribution function with decreasing T. At $T = 60$ °C, β_{KWW} in the PS microphase increases up to 0.63, exceeding also the value (~0.45) for bulk PMPS. Although a theoretical account for the β_{KWW} values in homopolymer melts is unknown so far, the systematic narrowing of the distribution function below T_g might be related to the spatial confinement[17] of PS segments due to reduction of V_f. With decreasing T, large V_f values and hence fast relaxation times would become less probable, resulting in a more symmetric and narrower distribution function. In contrast, the normal mode distribution of the polyisoprene (PI) block in the lamella phase of PS-*b*-PI copolymers[8] was found to be much broader than that of PI precursors. This broadening for $T > T_g$(PI) was ascribed to thermodynamic confinement to keep uniform overall segment density.

2. Low T_g Microphase. At low T, both experimental techniques can probe PMPS segmental dynamics and hence strengthen the extracted information for the PMPS microphase. As discussed in the data analysis, the utility of DS facilitates the analysis of the PCS experiment performed under partially heterodyne conditions. Both techniques yield experimentally the same values (Figure 4) for segmental orientation in the PMPS microregion; the dielectric strength for PS is very weak. The location of τ_f relative to the PMPS homopolymer in Figure 4 suggests microenvironments ($\sim V_c$) rich in PMPS (~96%). However, again the partitioning of the overall PMPS amount in these subvolumes, estimated from the dielectric $\Delta\epsilon$, is about 47%.

The width of the segmental distribution function is similar to that of the PMPS homopolymer. From the PCS experiment $\beta_{KWW} = 0.46 \pm 0.06$ which is virtually independent of T. Similarly the HN parameters α and γ for the $\epsilon''(\omega)$ spectrum correspond to $\beta_{KWW} = 0.46$ being also insensitive to T variations like the situation in bulk homopolymers. Recently,[6] in the disordered P(S-*b*-I) copolymer ($\chi N \simeq 9$) the width of the distribution function within the region rich in the low T_g component (PI) was also found to be independent of T. However, the parameter β_{KWW} ($\simeq 0.28 \pm 0.03$) assumed a lower value than in bulk PI ($\beta_{KWW} = 0.44$), probably due to the higher degree of mixing (~20% more PI). Conversely, in the present ordered system, the high concentration of PMPS within the PMPS microregions leads to distribution functions indistinguishable from that of pure PMPS. Finally, it is worth mentioning that a change in the T dependence of the fast relaxation time τ_f similar to that for the slow time τ_s would probably occur at even longer time scales inaccessible by either technique. The presence of PS in the PMPS microregion would shift the freezing of segmental fluctuations at smaller V_f values.

In summary, the microphase-separated P(S-*b*-MPS) displays two distinct segmental relaxation time scales similar to those of the two homopolymers. Within the region rich in the high T_g block, segmental orientation behaves differently than within the PMPS (low T_g component) microregion. In the present weakly segregated sample about 50% of the material is partitioned into the interphase region.

References and Notes

(1) Leibler, L. *Macromolecules* **1980**, *13*, 1602.
(2) Bates, F. S.; Fredrickson, G. H. *Annu. Rev. Phys. Chem.* **1990**, *41*, 525.
(3) Quan X.; Johnson, G. E.; Anderson, E. W.; Bates, F. S. *Macromolecules* **1989**, *22*, 245.
(4) Kanetakis, J.; Fytas, G.; Hadjichristidis, N. *Macromolecules* **1991**, *24*, 1806.
(5) Gerharz, B.; Fischer, E. W.; Fytas, G. *Polym. Commun.* **1991**, *32*, 469. Gerharz, B.; Vogt, S.; Fischer, E. W.; Fytas, G. *Colloid Polym. Sci.*, in press.
(6) Alig, I.; Fytas, G.; Kremer, F.; Roovers, J. *Macromolecules*, in press. Rizos, A.; Fytas, G.; Roovers, J. *J. Chem. Phys.*, in press.
(7) Kanetakis, J.; Fytas, G.; Kremer, F.; Pakula, T. *Macromolecules* **1992**, *25*, 3484.
(8) Yao, M. L.; Watanabe, H.; Adachi, K.; Kotaka, T. *Macromolecules* **1991**, *24*, 2955.
(9) Gerharz, B. Ph.D. Thesis, Max-Planck Institut für Polymerforschung, Mainz, Germany, 1991. Gerharz, B.; Wagner, Th.; Ballauff, M.; Fischer, E. W. *Polym. Commun.* **1992**, *33*, 3531.
(10) Ford, N. C., Jr. In *Dynamic Light Scattering*; Pecora, R., Ed.; Plenum Press: New York, 1985; see also references therein.
(11) Joosten, J. G. H.; McCarthy, J. L.; Pusey, P. N. *Macromolecules* **1991**, *24*, 6690.
(12) Havriliak, S.; Negami, S. *Polymer* **1967**, *8*, 161.
(13) Fischer, E. W.; Donth, E. J. W. *Phys. Rev. Lett.* **1992**, *68*, 2344 and references therein.
(14) Anastasiadis, S.; Russell, T. P.; Satiya, S. K.; Maykrzak, C. F. *J. Chem. Phys.* **1990**, *92*, 5677.
(15) Barrat, J. L.; Fredrickson, G. H. *J. Chem. Phys.* **1991**, *95*, 1981.
(16) Fried, H.; Binder, K. *J. Chem. Phys.* **1991**, *94*, 8349.
(17) Drake, J. M.; Klafter, J.; Levitz, P. *Science* **1991**, *251*, 1574.